

LA-UR-00-5969

Approved for public release;  
distribution is unlimited.

*Title:*

Probabilistic structural response of structure under  
collapse loading

*Author(s):*

J.E.Pepin, E.A.Rodriguez, B.H.Thacker and  
D.S.Riha

*Submitted to:*

<http://lib-www.lanl.gov/la-pubs/00796131.pdf>

Los Alamos National Laboratory, an affirmative action/equal opportunity employer, is operated by the University of California for the U.S. Department of Energy under contract W-7405-ENG-36. By acceptance of this article, the publisher recognizes that the U.S. Government retains a nonexclusive, royalty-free license to publish or reproduce the published form of this contribution, or to allow others to do so, for U.S. Government purposes. Los Alamos National Laboratory requests that the publisher identify this article as work performed under the auspices of the U.S. Department of Energy. Los Alamos National Laboratory strongly supports academic freedom and a researcher's right to publish; as an institution, however, the Laboratory does not endorse the viewpoint of a publication or guarantee its technical correctness.

# Probabilistic structural response of structure under collapse loading

J.E.Pepin & E.A.Rodriguez

*Los Alamos National Laboratory, Los Alamos, NM, USA*

B.H.Thacker & D.S.Riha

*Southwest Research Institute, San Antonio, TX, USA*

**ABSTRACT:** Engineers at Los Alamos National Laboratory (LANL) are currently developing the capability to provide a reliability-based structural evaluation technique for performing weapon reliability assessments. To enhance the analyst's confidence with these new methods, an integrated experiment and analysis project has been developed. The uncertainty associated with the collapse response of commercially available spherical marine float is evaluated with the aid of the non-linear explicit dynamics code DYNA3D (Whirley & Engelmann 1988) coupled with the probabilistic code NESSUS (Numerical Evaluation of Stochastic Structures Under Stress) (Thacker et al. 1998). Variations in geometric shape parameters and uncertainties in material parameters are characterized and included in the probabilistic model.

## 1 INTRODUCTION

Current arms control agreements have provided the impetus for national directives to cease production of new strategic weapons and end nuclear testing. This has placed a tremendous burden on the national laboratories for assuring stockpile certification. The Stockpile Stewardship Program's fundamental objective within the Department of Energy (DOE) is to maintain a high confidence in the safety, reliability, and performance of the existing U.S. nuclear weapons stockpile.

As such, enhanced evaluation capabilities are needed to determine the effect of possible anomalies that may arise in a weapon (e.g., due to aging mechanisms), and assess its performance, safety and overall reliability. Validated numerical methods must be employed in determining the reliability of specific weapon components, including the overall weapon system. The validated numerical models must, however, be based on accurate information of each component's geometry and material properties in an aged condition. Once these variables are known, extrapolation of potential lifetime of the weapon can be determined with some level of confidence. The goal is to develop an engineering capability that provides a reliability-based structural evaluation technique for performing weapon reliability assessments. To enhance the analyst's confidence with these new methods, an integrated experiment and analysis project has been developed.

The focus of this project is to generate precise probabilistic structural response simulations using

numerical models of commercially available, stainless steel spherical marine floats, under collapse loads, and compare with experimental results. The spherical marine float geometry was chosen because of its simple shape, yet highly complex nonlinear deformation behavior, leading to complex states-of-stress. There is also a wide variability associated with geometry and mechanical properties of commercially available (i.e., off-the-shelf) marine floats. The wide variability is not uncommon, and principally due to numerous forming processes, different operators, etc., which bulk production operations employ for a single material lot.

The probabilistic analysis is performed using the NESSUS probabilistic analysis software. NESSUS simulates uncertainties in loads, geometry, material behavior, and other user-defined uncertainty inputs to compute reliability and probabilistic sensitivity measures. To facilitate analyses of a broad range of problem types, a large number of efficient and accurate probabilistic methods are included in NESSUS. The probabilistic validation of the current work is performed in two phases. Initially, the deterministic spherical marine float model is validated against the experimentally observed collapse load. Next, variations in geometric shape parameters (i.e., surface geometry and thickness) are characterized using test data from actual float geometry. Uncertainties in material properties (i.e., stiffness, strength, and flow) are also included in the probabilistic model. Finally, the probabilistic numerical model is validated by comparison to the predicted and observed variation in collapse load.

## 2 DESCRIPTION OF MARINE FLOAT

The structural components are “off-the-shelf,” commercially available, marine floats commonly used by the petro-chemical industries in large open, or closed, tanks for liquid level (gage) measurements. The marine floats were purchased directly from Quality Float Works in Shaumburg, IL, with a 9-inch outside diameter, 16-gage shell thickness, and no optional external piping connection. The goal was to obtain spherical shapes with as little as possible of any external structural perturbations, such as connections, thus limiting the complexity in collapse behavior. Nevertheless, each float has a small closure connection at the north pole that is used a final seal. For the experimental collapse process, the north pole seal is drilled to release entrapped air during compression.

No information was available from the manufacturer relative to whether the 100 floats purchased were from a single, or different, material lot. Also, because many liquids used in the petro-chemical industry are corrosive to metals, the choice material for marine floats is stainless steel, Type 316 or 304L. This is also fortuitous since 304L stainless steel is a well known and characterized material in the commercial nuclear industry. This implies that statistical variations in mechanical properties are readily available and may be used to compare with actual float characterization. However, actual material testing of a specified set of floats would provide better information on the variations within a single float, among several floats, and possibly within a material lot.

Small compression coupons, taken from a single marine float, were tested to determine their mechanical properties and also obtain a measure of their variation. Figure 1 shows the number of coupons, and the region, where the samples were taken. Although, the figure shows numerous samples taken from one region, the samples were actually taken from the complete periphery (i.e., 360°). This allows a better approximation of the variation in properties throughout the float. Table 1 shows the results of the compression tests compared to “as-received” 304L in plate stock.

Table 1. Mechanical properties.

	$S_y$ ksi	$S_u$ ksi	n
304L as-received	32.0	75.0	0.25
Weld	51.0	88.5	0.28
Center (equatorial)	123.0	170	0.10
Middle	77.0	117	0.22
Top	68.5	118	0.23

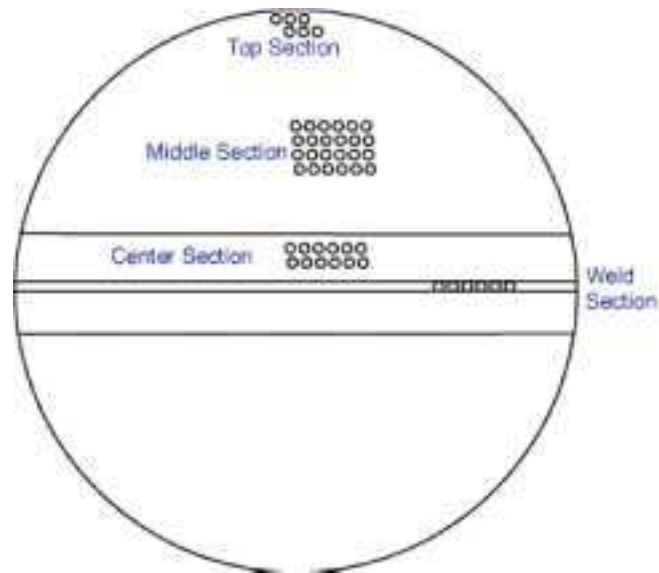


Figure 1. Compression coupons locations.

Figure 2 shows the typical true stress-true strain curves for the different sections of the marine float. It is evident from Table 1 that extensive cold-work has been applied to the hemispherical shells, especially within the equatorial region. Figure 3 provides a measure of mechanical properties as a function of cold-work, suggesting that the equatorial region has received approximately 50% cold-work. This has been confirmed in discussions with the manufacturer, such that the drawing (or hydraulic pressing) process applies slightly higher cold-work on the flat sheet stock around the equatorial region.

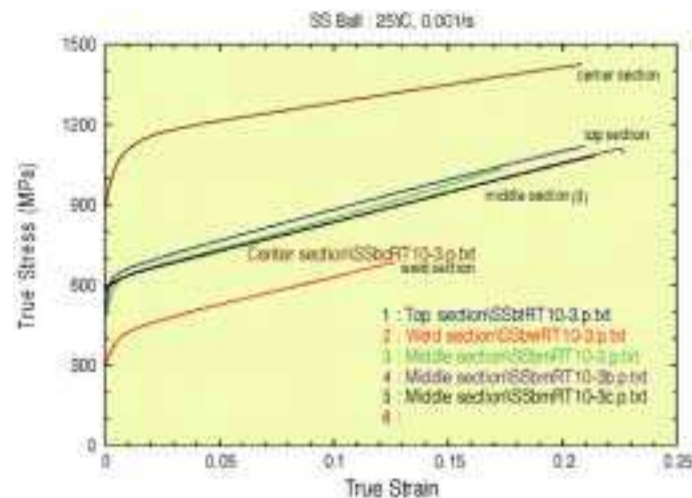


Figure 2. Stress strain data.

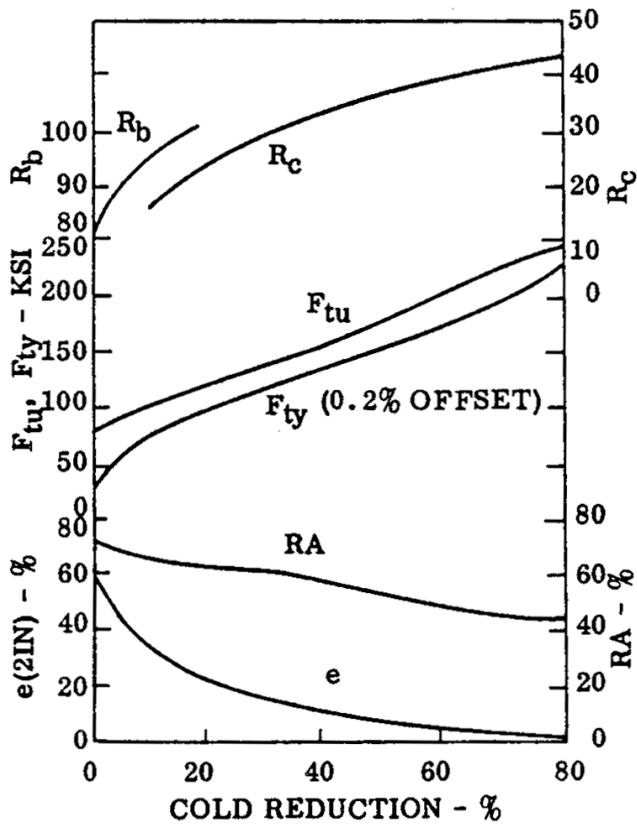


Figure 3. Effect of cold-work on 304L (Holt 1992).

As previously stated, the floats are drawn into hemispherical shells from flat circular plate stock using a hydraulic press. The flat plate stock would have the nominal mechanical properties for common 304L plate/sheet. Once the hemispherical shells are pressed, each hemisphere is placed upon an automatic turning fixture for welding. Gas tungsten arc welding (GTAW), or commonly termed “tungsten inert gas” (TIG), is employed with helium as the shield gas to maintain an uncontaminated weld. The hemispheres are then welded at the equator, from the outside only, applying a 1/8-inch bead in a continuous process.

### 3 DETERMINISTIC ANALYSIS

#### 3.1 Model

The simulation of a marine float being crushed between two platen strokes was performed using DYNA3D, a nonlinear, explicit, Lagrangian finite element analysis code for three-dimensional transient structural mechanics. The float was meshed with 15,600 quadrilateral shell elements into three

distinct regions, the weld, a center band, and poles. The three regions are necessary in order to use different constitutive models to accurately model the mechanical behavior of the steel. A tabular elastic-plastic material model was used to model each region. The measured true stress, true strain curves as well as the elastic-plastic models are shown in Figure 5. A single hexahedral element was used to mesh each of the platens. The platens are modeled as rigid body material. The bottom platen is held fixed and the top platen is given a constant velocity to crush the float.

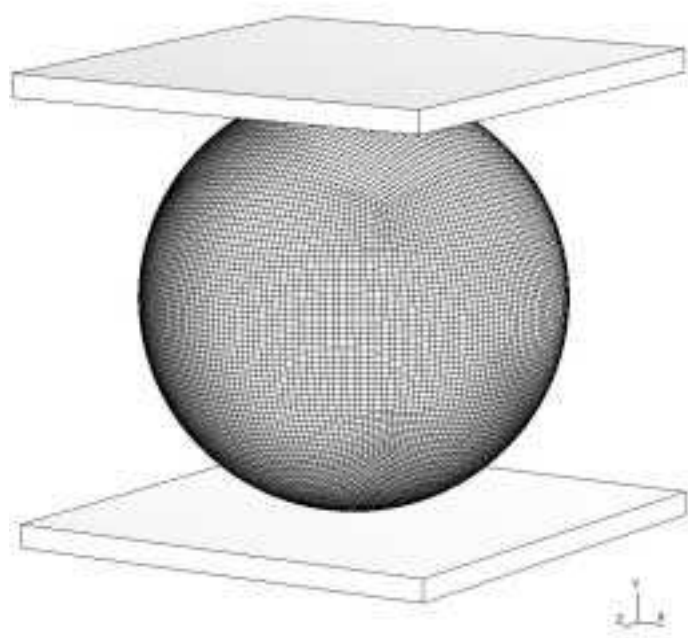


Figure 4. The mesh used for the marine float and platens.

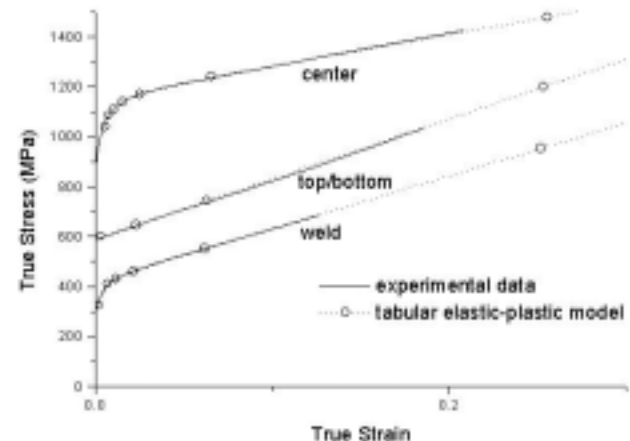


Figure 5. Stress-strain curves used to represent the SS304L material behavior.

### 3.2 Results

As an explicit finite element code, DYNA3D uses a large number of extremely small time steps to solve the governing equations for any given problem. This makes DYNA3D an efficient and ideal code for simulating transient events that occur in fractions of a second. The float, however, is crushed at 2 in/s. When simulating this quasi-static event, a compromise must be made between crush velocity and computational efficiency. Figure 6 shows the force required to crush the float for three different velocities. When the top platen is moving down at 10 m/s, a significant amount of dynamic noise can be seen in the force curve for the first 4.5 inches followed by a sharp spike up to 75,000 pounds at 5.5 inches. At 5 and 1 m/s, the dynamic noise has disappeared and the analysis is converging on a solution. Although the 1 m/s analysis may be a better quasi-static solution, it takes approximately 8 days, or 192 hours, of cpu time on a single processor to run. The 5 m/s analysis provides the best compromise between computational efficiency and a quasi-static solution. The solution is similar to the 1 m/s case and uses only 2 days of cpu time. Because a probabilistic analysis requires several simulations to be run as random variables are perturbed, it was decided to use the 5 m/s case as the nominal, or mean value, analysis.

To date, twelve floats have been crushed experimentally. The load deflection curves for these floats are plotted with the nominal, 5 m/s, analysis in Figure 7. The hydraulic press used to crush the floats has a maximum stroke of four inches. As such, the floats must be crushed in two steps resulting in the unloading and then reloading seen between 3.5 and 4 inches. The force required to crush the floats is slightly higher than calculated for the first 4.5 inches. Since the two hemispheres for each float are pressed from flat plates, there is an increase in work hardening from the pole down to the equator. It is reasonable to assume that there is a gradual increase in material strength from the pole to the equator. The analysis assumes a discontinuous jump in material strength based on the limited testing of one float as described above. At 4.5 inches, the platens have crushed the finite element model to the higher strength center band. From this point on, the calculated force closely matches the force curves found from experiment.

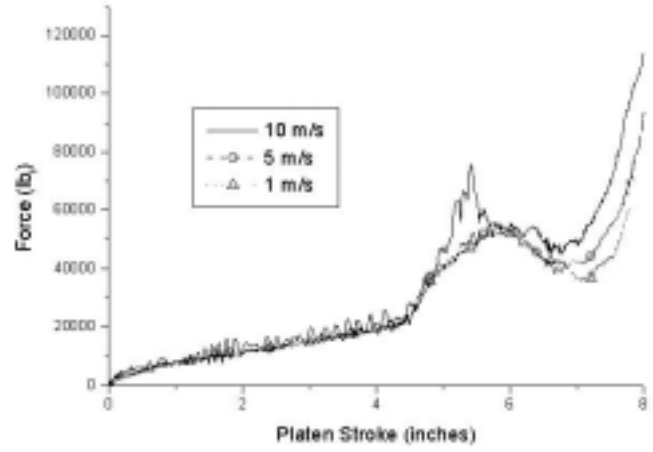


Figure 6. Force required to crush the float at three different velocities.

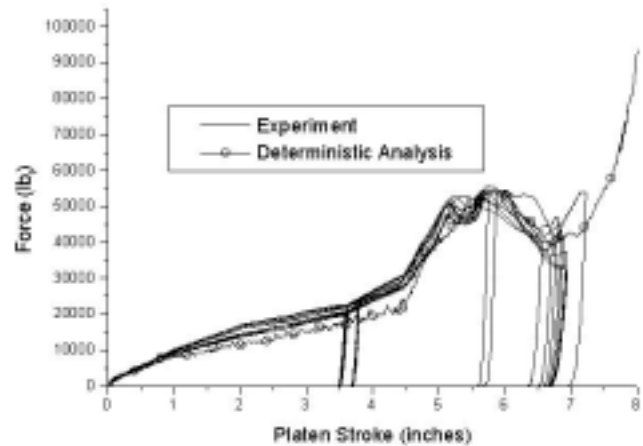


Figure 7. Comparison of experimental and deterministic force v. stroke curve.

A comparison between one of the crushed floats and the analysis can be made in Figure 8. During the experiment, the floats were consistently crushed into five lobes. The analysis displays similar buckling characteristics except that only four lobes develop. Unlike the actual floats, the finite element model is based on the geometry of a perfect sphere. Slight inconsistencies in geometry and material properties that can easily arise from the manufacturing process are not incorporated in the model. It is believed that these small differences can result in a sphere being crushed into five lobes as opposed to four. It is clear from a cursory look at the deterministic analysis that the complicated structural response of the floats is not entirely incorporated in the model. In this case, the purpose of a probabilistic analysis is to define a response surface and develop a better understanding of the mechanical behavior of the float.



Figure 8. Comparison of experiment with deterministic analysis at a platen stroke of 7 inches.

## 4 PROBABILISTIC ANALYSIS

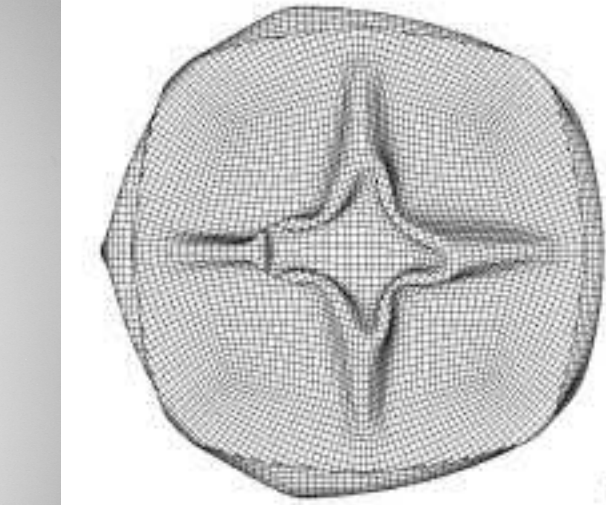
### 4.1 Methods

Efficient probabilistic methods were used to calculate the probabilistic response of the float crush (Wu & Burnside 1988). These methods have been primarily developed for complex computational systems requiring time-consuming calculations, the results of which have been shown to approach the exact solution obtained from tradition Monte Carlo methods using significantly fewer function evaluations (Thacker et al. 1991).

#### 4.1.1 Most probable point

A class of probabilistic methods based on the most probable point (MPP) are becoming routinely used as a means of reducing the number of g-function evaluations from that of brute-force Monte Carlo simulation. Although many variations have been proposed, the best-known and most widely-used MPP-based methods include the first-order reliability method (FORM) (Thacker et al. 1991), second-order reliability method (SORM) (Thacker et al. 1991), and advanced mean value (AMV) (Wu et al. 1990).

The basic steps involved in MPP-based methods are as follows: (1) Obtain an approximate fit to the exact g-function at  $X^*$ , where  $X^*$  is initially the mean random variable values; (2) Transform the original, non-normal random variables into independent, normal random variables  $u$  (Thacker et al. 1991); (3) Calculate the minimum distance,  $\beta$  (or



safety index), from the origin of the joint PDF to the limit state surface,  $g = 0$ . This point,  $u^*$ , on the limit state surface is the most probable point (MPP) in the  $u$ -space; (4) Approximate the  $g$ -function  $g(u)$  at  $u^*$  using a first or second-order polynomial function; and (5) Solve the resulting problem using available analytical solutions (Thacker et al. 1991).

Step (1), which involves evaluating the  $g$ -function, represents the main computational burden in the above steps. Once a polynomial expression for the  $g$ -function is established, it is a numerically simple task to compute the failure probability and associated MPP. Because of this, the complete response CDF can be computed very quickly by repeating steps (2)-(4) for different  $z_0$  values. The resulting locus of MPP's is efficiently used in the advanced mean value algorithm (discussed next) to iteratively improve the probability estimates in the tail regions.

#### 4.1.2 Advanced mean value

The advanced mean value class of methods are most suitable for complicated but well-behaved response functions requiring computationally-intensive calculations. Assuming that the response function is smooth and a Taylor's series expansion of  $Z$  exists at the mean values, the mean value  $Z$ -function can be expressed as:

$$Z_{MV} = Z(\mu) + \sum_{i=1}^n \frac{\partial Z}{\partial X_i} \Big|_{\mu_i} (X_i - \mu_i) + H(\mathbf{X}) \quad (1)$$

where  $Z_{MV}$  is a random variable representing the sum of the first order terms and  $H(\mathbf{X})$  represents the higher-order terms.

For nonlinear response functions, the MV first-order solution obtained by using Equation 1 may not be sufficiently accurate. For simple problems, it is

possible to use higher-order expansions to improve the accuracy. For example, a mean-value second-order solution can be obtained by retaining second-order terms in the series expansion. However, for problems involving implicit functions and large  $n$ , the higher-order approach becomes difficult and inefficient.

The AMV method improves upon the MV method by using a simple correction procedure to compensate for the errors introduced from the truncation of the Taylor's series. The AMV model is defined as:

$$Z_{AMV} = Z_{MV} + H(Z_{MV}) \quad (2)$$

where  $H(Z_{MV})$  is defined as the difference between the values of  $Z_{MV}$  and  $Z$  calculated at the Most Probable Point Locus (MPPL) of  $Z_{MV}$ , which is defined by connecting the MPP's for different  $z_0$  values. The AMV method reduces the truncation error by replacing the higher-order terms  $H(X)$  by a simplified function  $H(Z_{MV})$ . As a result of this approximation, the truncation error is not optimum; however, because the  $Z$ -function correction points are usually close to the exact MPP's, the AMV solution provides a reasonably good solution.

The AMV solution can be improved by using an improved expansion point, which can be done typically by an optimization procedure or an iteration procedure. Based initially on  $Z_{MV}$  and by keeping track of the MPPL, the exact MPP for a particular limit state  $Z(X) - z_0$  can be computed to establish the AMV+ model, which is defined as:

$$Z_{AMV+} = Z(\mathbf{X}^*) + \sum_{i=1}^n \frac{\partial Z}{\partial X_i} \Big|_{X_i^*} (X_i - \chi_i^*) + H(\mathbf{X}) \quad (3)$$

where  $\mathbf{X}^*$  is the converged MPP. The AMV-based methods have been implemented in NESSUS and validated using numerous problems (Thacker et al. 1991, Wu et al. 1990).

## 4.2 Probabilistic sensitivities

For design purposes, it is important to know which problem parameters are the most important and the degree to which they control the design. This can be accomplished by performing sensitivity analyses. In a deterministic analysis where each problem variable is single-valued, design sensitivities can be computed that quantify the change in the performance measure due to a change in the parameter value, i.e.,  $\partial Z / \partial X_i$ .

As stated earlier, each random input variable is characterized by a mean value, a standard deviation, and a distribution type. That is, three parameters are defined as opposed to just one. The performance measure is the injury probability (or safety index).

Sensitivity measures are needed then to reflect the relative importance of each of the probabilistic parameters on the probability of injury. NESSUS computes probabilistic based sensitivities for both MPP and sampling based methods (Thacker et al. 1991). The sensitivity computed as a by-product of MPP-based methods is:

$$\alpha_i = \frac{\partial \beta}{\partial u_i} \quad (4)$$

which measures the change in the safety index with respect to the standard normal variate  $u$ . Although useful for providing an importance ranking, this sensitivity is difficult to use in design because  $u$  is a function of the variable's mean, standard deviation, and distribution. Two other sensitivities that are more useful for design (and for importance ranking as well) include:

$$S_\mu = \frac{\partial p_I}{\partial \mu_i} \frac{\sigma_i}{p_I} \quad (5)$$

which measures the change in the probability of injury with respect to the mean value; and:

$$S_\sigma = \frac{\partial p_I}{\partial \sigma_i} \frac{\sigma_i}{p_I} \quad (6)$$

which measures the change in the probability of injury with respect to the standard deviation. Multiplying by  $\sigma_i$  and dividing by  $p_I$  nondimensionalizes and normalizes the sensitivity to facilitate comparison between variables. The sensitivities given by Equations 5 and 6 are computed for both component and system probabilistic analysis.

## 4.3 Probabilistic response of float

In order to capture, as simply as possible, the total structural response of a float under collapse, it was decided to perform a probabilistic analysis at the point of maximum force during buckling. The maximum force needed to crush the float occurs at a platen stroke of approximately 6 inches. For the first 4.5 inches, the top and bottom of the float dimple inward. The float is buckling for the next 1.5 inches leading up to the point of maximum force. After this point, the float will be compressed to such an extent that it begins to act like a solid piece of steel between the two platens.

Table 2. Probabilistic data for the random variables.

Random variable	PDF	COV
$E$	Lognormal	0.0238
$S_v$	Normal	0.10

Radius	Normal	0.00158
Thickness	Normal	0.00158

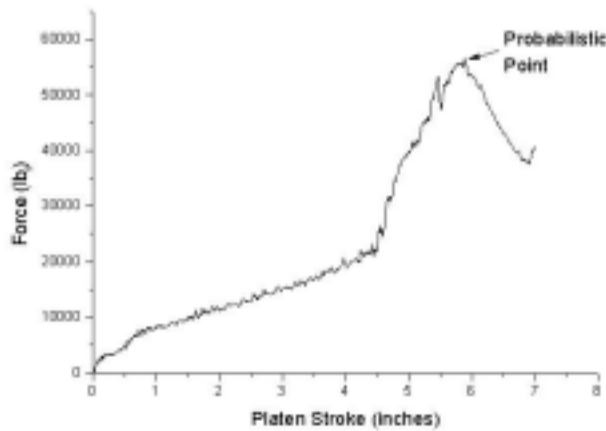


Figure 9. Point used for probabilistic analysis.

To date, a comprehensive investigation of float geometry and material characteristics has not been accomplished. The outside contours of all the floats, however, have been measured and statistical data on the radius is available. Due to this lack of statistical data, a simple probabilistic analysis has been done using four random variables and applying rules-of-thumb where appropriate. The random variables for this analysis are modulus of elasticity, yield stress, radius, and thickness of the steel plate. The coefficients of variation (COV) for modulus of elasticity and yield stress are taken from a handbook (Haugen 1980) for 304 stainless steel. The COV for radius was calculated from the outside contour information. An assumption is made that the manufacturing tolerance for the thickness of the steel plates is equivalent to the radius tolerance. Therefore, the COV's for thickness and radius are equal.

The CDF of the response function was calculated using NESSUS and plotted in x- and u-space. Figure 10 shows the sensitivity of the random variables with regard to the calculation. Figures 11 and 12 show the results from the Mean Value and Advanced Mean Value analyses. A limited Monte Carlo analysis using twenty sampling points has been included to validate the results.

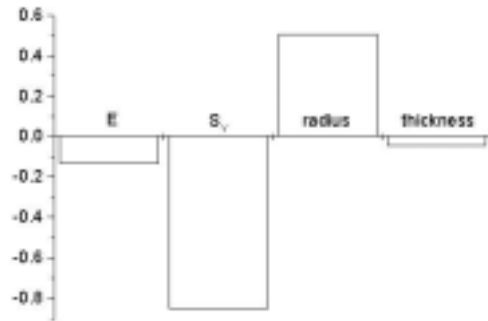


Figure 10. Sensitivity factors ( $\alpha$ ) of the random variables.

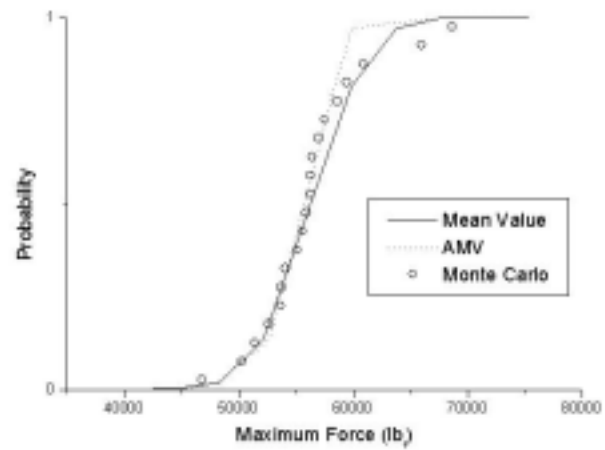


Figure 11. CDF of the response function.

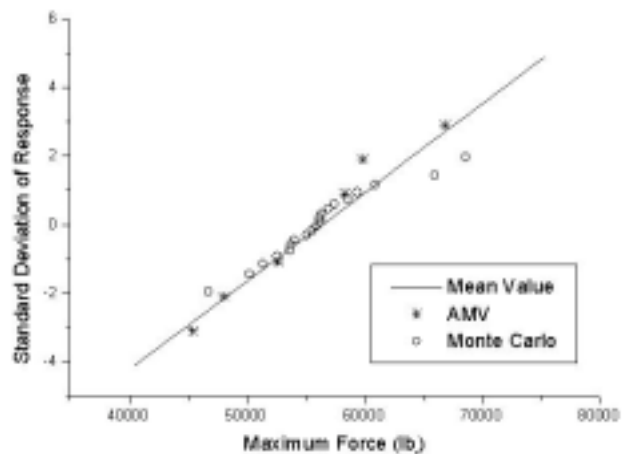


Figure 12. CDF of the response function in u-space.

The Mean Value method, a simple, linear approximation of the response about the mean, matches nicely with the twenty Monte Carlo points. The Advanced Mean Value method is a perturbation about the MV solution and is intended to improve the solution about the tails of the CDF. In this case, the upper tail of the AMV solution seems to diverge

from the Monte Carlo samples. Although not thoroughly investigated at this point, it is currently believed that small perturbations in the random variables can occasionally alter the buckling characteristics of the float. A change in the buckling pattern can result in different structures that could weaken or strengthen the float. This phenomenon can cause the response function to be non-linear. The AMV solution will be susceptible to nonlinearities in the response. There has been no attempt at this time to refine the solution with further perturbations of the AMV solution or application of the AMV+ method.

## 5 CONCLUSION

The probabilistic analysis documented here demonstrates the power and usefulness of NESSUS. Using the efficient algorithms of the Mean Value method can provide valuable insight above and beyond the deterministic analysis. A range of buckling loads has been determined and the importance of the dependent variables on the maximum buckling load can be examined.

The question remains on the appropriateness of using the maximum buckling load as the response function for this problem. Further investigation is needed to determine conclusively if perturbations in the dependent variables are causing a non-linear response in the buckling load. Additionally, a better understanding of the different buckling characteristics of the float is required. Also, it may be necessary to consider using a response function other than the maximum buckling force, such as the total work done in crushing.

Finally, once a proper interrogation of float geometry and material has been accomplished and statistical data is available, a more detailed and accurate probabilistic analysis will be completed. Currently, the thickness of the steel plates is taken to be constant throughout each hemisphere. If statistical data finds thickness to vary from equator to pole in terms of mean, standard deviation, and type of PDF, this information can be incorporated in the model.

## ACKNOWLEDGEMENT

This work was performed by Los Alamos National Laboratory under Contract No. W-7405-ENG-36 with the US Department of Energy (DOE).

Holt, J.M. (technical editor) 1992. *US Air Force Structural Alloys Handbook, Vol. 2*. CINDAS/Purdue University.

Thacker, B.T. et al. 1991. Computational Methods for Structural Load and Resistance Modeling. *AIAA Journal, Vol. 2, No. 9*, September.

Thacker, B.T. et al. 1998. *NESSUS User's Manual*. Southwest Research Institute.

Whirley, R. & Engelmann, B. 1988. *DYNA3D User Manual*. Lawrence Livermore National Laboratory report UCRL-MA-107254, Rev. 1, December.

Wu, Y.T. & Burnside, O.H. 1988. Efficient Probabilistic Structural Analysis Using An Advanced Mean Value Method. *Proceedings, ASCE Specialty Conference on Probabilistic Mechanics*.

Wu, Y.T. et al. 1990. Advanced Probabilistic Structural Analysis Method for Implicit Performance Functions. *AIAA Journal, Vol. 2, No. 9*, September.

## REFERENCES

Haugen, E.B. 1980. *Probabilistic Mechanical Design*. Wiley.